

# Simultaneous dual free spectral range microwave photonic filter using a high-birefringence chirped grating in a Sagnac loop

Guoxiang Ning, Ping Shum, and Sheel Aditya

*Network Technology Research Centre, Nanyang Technological University, 50 Nanyang Drive, Research Techno Plaza, 4th Story, Slab Block, Singapore 637553*

Yandong Gong

*Innovation Centre, Institute for InfoComm Research, Nanyang Drive, Singapore 637723*

Received May 31, 2006; revised July 26, 2006; accepted July 28, 2006;  
posted August 3, 2006 (Doc. ID 71566); published December 13, 2006

We propose a continuously tunable, dual free spectral range (FSR) photonic microwave notch filter configuration using a high-birefringence linearly chirped fiber Bragg grating (Hi-Bi LCFBG) that is connected in a Sagnac loop using a Hi-Bi coupler. The configuration employs double sideband modulation and can generate two FSRs simultaneously. The larger FSR corresponds to the differential time delay of the Hi-Bi LCFBG and the Hi-Bi pigtailed of the coupler; the smaller FSR corresponds to the time delay between the arms of the Sagnac loop. Measured results demonstrate dual FSR, a large notch rejection, and that the FSR is easily tunable by tuning the LCFBG. We also present the filter transfer function for the design. Experimental results agree well with the theoretical analysis. © 2006 Optical Society of America

*OCIS codes:* 350.2460, 350.4010, 060.2310.

## 1. INTRODUCTION

There are many advantages of microwave signal transmission and processing directly in the optical domain such as large time–bandwidth products, immunity to electromagnetic interference, reduced size and weight, and low and constant electrical loss. Many filters and signal processing structures using fiber Bragg gratings (FBG) have been reported in the literature.<sup>1,2</sup> A very useful component in rf systems is a tunable notch filter with a high resolution. To achieve microwave signal processing by optical means, optically incoherent summing of two light beams should be achieved. This requires low coherence sources, which can accommodate a large free spectral range<sup>3,4</sup> (FSR); however, these optical sources will reduce the available bandwidth of a photonic microwave system. Many filters and signal processing structures were proposed in Refs. 1 and 5. Recently, an optically incoherent operation using high birefringence (Hi-Bi) FBGs in a transversal filter has been reported,<sup>6</sup> but this design is restricted to step tuning. A continuously tunable design using a Hi-Bi chirped grating has also been reported<sup>7</sup>; unfortunately, it needs a polarization beam splitter, which has a poor signal-to-noise ratio (SNR). Most significantly, the notch filter designs reported so far provide only one value of the FSR at a given instant of time.

We propose here a continuously tunable photonic microwave notch filter configuration. The filter uses a Sagnac loop containing a Hi-Bi linearly chirped FBG (LCFBG). The Hi-Bi LCFBG is connected between two

arms of a polarization maintaining (PM)  $2 \times 2$  50:50 fiber coupler. The filter provides two values of FSR simultaneously. The larger FSR corresponds to the differential group delay (DGD) of the Hi-Bi LCFBG and the Hi-Bi pigtailed of the coupler, while the smaller one is caused by the Sagnac loop interferometer. Measured experimental results demonstrate the dual-FSR property as well as the tunability of the FSR.

## 2. FILTER CONFIGURATION AND OPERATION PRINCIPLE

The experimental setup for the proposed microwave filter is shown in Fig. 1. An rf signal (40 MHz to 10 GHz) drives an electro-optic amplitude modulator (EOM) with PM pigtailed at both the output and the input ports, which modulates the output of a laser with a linewidth of 100 MHz. The output of the EOM is launched into a  $\lambda/4$  wave plate, which changes the input state of polarization (SOP). The signal passes through an isolator and then, through a 3 dB Hi-Bi coupler, it is coupled into a Sagnac loop, which includes a Hi-Bi LCFBG. The slow and fast axes of the LCFBG are aligned with the slow and fast axes, respectively, of the pigtailed of the 3 dB Hi-Bi coupler. The wave plate is adjusted to excite the two orthogonal SOPs of the Hi-Bi LCFBG equally. The output of the Sagnac loop is fed into a photodetector, which is followed by a network analyzer. With this design, the detected signal is expected to exhibit two FSRs.

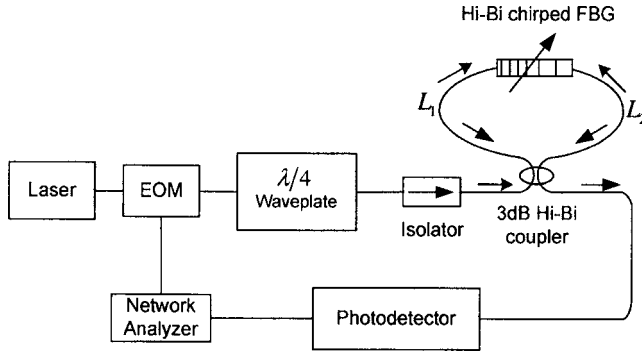


Fig. 1. Experimental setup.

The larger FSR is induced by the DGD of the Hi-Bi LCFBG and the Hi-Bi pigtails of the coupler. The Hi-Bi LCFBG has two almost identical stop bands corresponding to the two orthogonal polarization axes, fast and slow. For a given signal wavelength, which is in the common bandwidth of the two stop bands, after the signal is reflected by the grating, a certain amount of DGD occurs between the fast and slow axes.

The smaller FSR is caused by the Sagnac loop interferometer. The path difference between the two arms of the Sagnac loop interferometer consists of two contributions: one is the length difference between  $L_1$  and  $L_2$  (which causes fixed time delay), and the other comes from the chirped grating. The fixed time delays for the fast and slow axes due to the length difference can be expressed as  $\Delta\tau_{s0} = 2\beta_{s1}L_2 - 2\beta_{s1}L_1$  and  $\Delta\tau_{f0} = 2\beta_{f1}L_2 - 2\beta_{f1}L_1$ , where  $\beta_{s1} = (\partial\beta_s/\partial\omega)|_{\omega=\omega_0}$ ,  $\beta_{f1} = (\partial\beta_f/\partial\omega)|_{\omega=\omega_0}$ , and  $\beta_s(\omega)$  or  $\beta_f(\omega)$  is the propagation constant for the corresponding axis. The time delay caused by the chirped grating for a signal incident on the short wavelength port is  $(2n_{\text{eff}}z/c) - d_\rho\Delta\lambda$ ,<sup>8</sup> where  $n_{\text{eff}}$  is the effective refractive index for the grating,  $z$  is the position of reflection on the chirped grating depending on the Bragg wavelength  $\lambda_D$ ,  $d_\rho = (2n_{\text{eff}}/c)(d\lambda_D/dz)^{-1}$ , and  $\Delta\lambda$  is the chirped wavelength depending on the modulation frequency  $\omega_m$ . For simplicity, in this part we assume that the grating parameters  $n_{\text{eff}}$ , etc., are approximately the same for the two orthogonal axes. Similarly, the time delay caused by the chirped grating for a signal incident on the long wavelength port is  $[2n_{\text{eff}}(l-z)/c] + d_\rho\Delta\lambda$ , where  $l$  is the length of the Hi-Bi LCFBG. This smaller FSR superimposes on the larger one described earlier.

The transfer function for the microwave filter, when the signal SOP is completely aligned with the fast or slow axis, can be expressed as

$$|H_{s(f)}(\omega_m)| = \frac{RM^2}{2} \cos(d_\rho\omega_m^2\lambda^2/4\pi c) \times \left| \exp\left\{-j\left[\frac{2n_{\text{eff}}z}{c} + 2\beta_{s1(f1)}L_1\right]\omega_m\right\} + \exp\left\{-j\left[\frac{2n_{\text{eff}}(l-z)}{c} + 2\beta_{s1(f1)}L_2\right]\omega_m\right\} \right|, \quad (1)$$

where  $R$  is the responsivity of the photodetector and  $M$  is a magnitude factor. When the SOPs corresponding to the

fast and slow axes are excited equally, the transfer function can be shown to be

$$|H(\omega_m)| = |H_s(\omega_m) + H_f(\omega_m)| = \frac{RM^2}{2} \cos(d_\rho\omega_m^2\lambda^2/4\pi c) \times \left| \exp\left[-j\left(\frac{\Delta\tau_{df} + \Delta\tau_{d0}}{2}\right)\omega_m\right] + \exp\left[-j\left(-\frac{\Delta\tau_{df} + \Delta\tau_{d0}}{2}\right)\omega_m\right] \right| \times \left| \exp\left\{-j\left[\frac{2n_{\text{eff}}z}{c} + 2\beta_{f1}L_1\right]\omega_m\right\} + \exp\left\{-j\left[\frac{2n_{\text{eff}}(l-z)}{c} + 2\beta_{f1}L_2\right]\omega_m\right\} \right|. \quad (2)$$

In Eq. (2), the magnitude of the filter response function consists of a product of two factors: (i)  $\cos(d_\rho\omega_m^2\lambda^2/4\pi c)$  and (ii)  $|\cos[\omega_m(\Delta\tau_d/2)]\cos[\omega_m(\Delta\tau/2)]|$ , where  $\Delta\tau_d = \Delta\tau_{df} + \Delta\tau_{d0}$ .  $\Delta\tau_{df}$  denotes the DGD owing to the Hi-Bi LCFBG;  $\Delta\tau_{d0}$  is the DGD owing to the pigtails of the Hi-Bi coupler and is equal to DGD per meter for the PM fiber ( $\sim 1.67$  ps/m) multiplied by  $(2L_1 - 2L_2)$ .  $\Delta\tau = \Delta\tau_{f0} + [2n_{\text{eff}}(l-z)]/c - 2n_{\text{eff}}z/c$ . The second factor clearly shows that the filter is capable of generating two FSRs simultaneously. Further, Eq. (1) shows that if the input SOP is aligned to the fast or the slow axis of the Hi-Bi LCFBG, the filter becomes a single FSR filter, similar to those in Refs. 4 and 9; this FSR value can be switched between two values corresponding to one of the two orthogonal axes.

### 3. EXPERIMENTAL RESULTS AND DISCUSSION

The Hi-Bi LCFBG was written by exposing a hydrogen-loaded Hi-Bi fiber to a 244 nm laser beam through a linearly chirped phase mask. The Hi-Bi LCFBG has a 10% apodization area at both sides of the grating to suppress the ripple of group delay in the bandwidth. The length of the grating is  $\sim 7$  cm. The reflectivities for the fast and slow axes are shown in Fig. 2. The figure clearly shows that the reflection spectra for the fast and slow axes are almost identical with 0.4 nm wavelength separation. The 3 dB bandwidth for each stop band is  $\sim 1.504$  nm. The measured DGD for the Hi-Bi LCFBG is shown in Fig. 3. The DGD value is  $\sim 196$  ps in the overlap bandwidth. The lengths of arm 1 ( $L_1$ ) and arm 2 ( $L_2$ ) are 2.329 and 0.6 m, respectively. Therefore, the DGD owing to the Hi-Bi pigtails,  $\Delta\tau_{d0}$ , is  $\sim 6$  ps. The total DGD ( $\Delta\tau_d$ ) is  $\sim 202$  ps, which corresponds to a calculated value of 2.475 GHz for the first notch frequency for the larger FSR. Figure 4(a) shows the measured response of the filter demonstrating two simultaneous values of FSR, with the first notch frequency of the envelope at  $\sim 2.45$  GHz. The larger FSR, which is measured by disconnecting arm 2 of the Sagnac interference loop and shown in Fig. 4(b), is approximately  $2 \times 2.49$  GHz. When arm 2 in Fig. 1 is disconnected, one

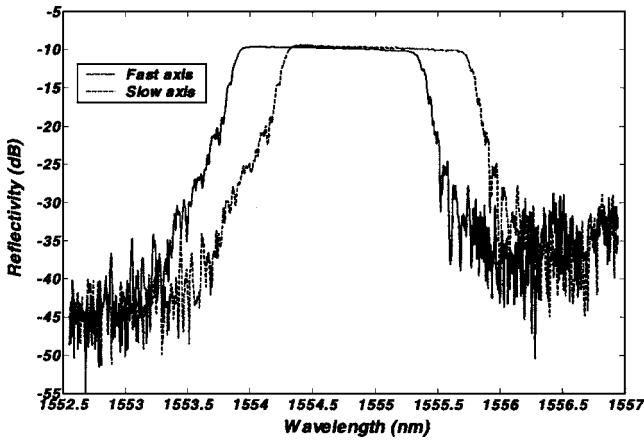


Fig. 2. Hi-Bi LCFBG reflectivity for the fast axis and the slow axis.

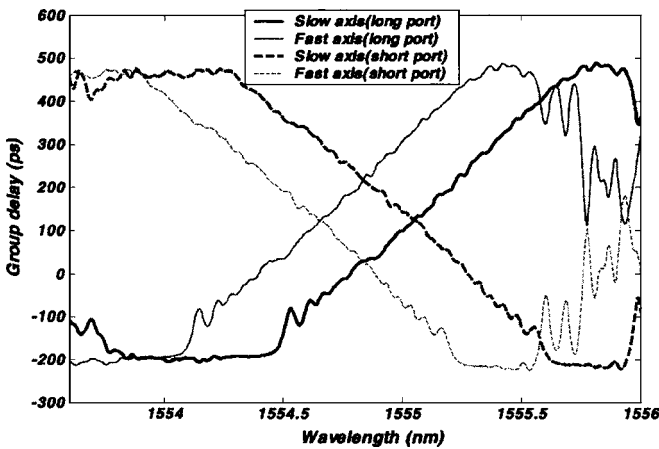


Fig. 3. Measured DGD for Hi-Bi LCFBG.

still gets two optically uncorrelated signals at the photo-detector corresponding to the slow and fast axes of the Hi-Bi pigtailed and the Hi-Bi LCFBG. These two signals interfere to form the filter response. The measured results for the larger FSR agree well with the calculated result.

Figure 4(c) shows the measured filter response expanded at  $\sim 5$  GHz, clearly showing the smaller FSR. A FSR of 57.86 MHz and a notch rejection of more than 30 dB are obtained. The estimated time delay  $\Delta\tau$  is  $\sim 17,290$  ps corresponding to the lengths of arms 1 and 2 mentioned earlier; this corresponds to a FSR of 57.84 MHz. The discrepancy between the measured and calculated FSR values is less than 1%. The coherence time for the laser source is  $\sim 10$  ns, which is smaller than  $\Delta\tau$ . Therefore, the filter operation is free from the problem of optical coherence, and the response of the filter is very stable.

The FSRs can be tuned by linearly tuning the chirped grating with a beam.<sup>10</sup> Figures 5(a)–5(c) show the measured filter responses when the operation of the grating is shifted to a wavelength shorter by 0.1 nm. The first notch frequency of the envelope is  $\sim 2.41$  GHz [Fig. 5(a)], the larger FSR is approximately  $2 \times 2.44$  GHz [Fig. 5(b)], and the smaller FSR is 57.53 MHz [Fig. 5(c)].

Measured and calculated FSR values for different shifts in the operating wavelength of the FBG are shown

in Fig. 6. Our experimental results agree well with the calculated results based on theory. For the calculated results for the smaller FSR, the time delay is 17,290 ps, and the equation used is  $FSR_{sm} = 10^6 / [17,290 - (2x/1.504) \times 700]$  (MHz). The calculated larger FSR is  $2 \times 2.475$  GHz corresponding to a DGD of 202 ps. If one uses multiple laser sources, the present filter design can be extended to a higher number of taps. Also, a filter with tunable tap weights can be realized by using a tunable Hi-Bi coupler instead of the 3 dB Hi-Bi coupler.

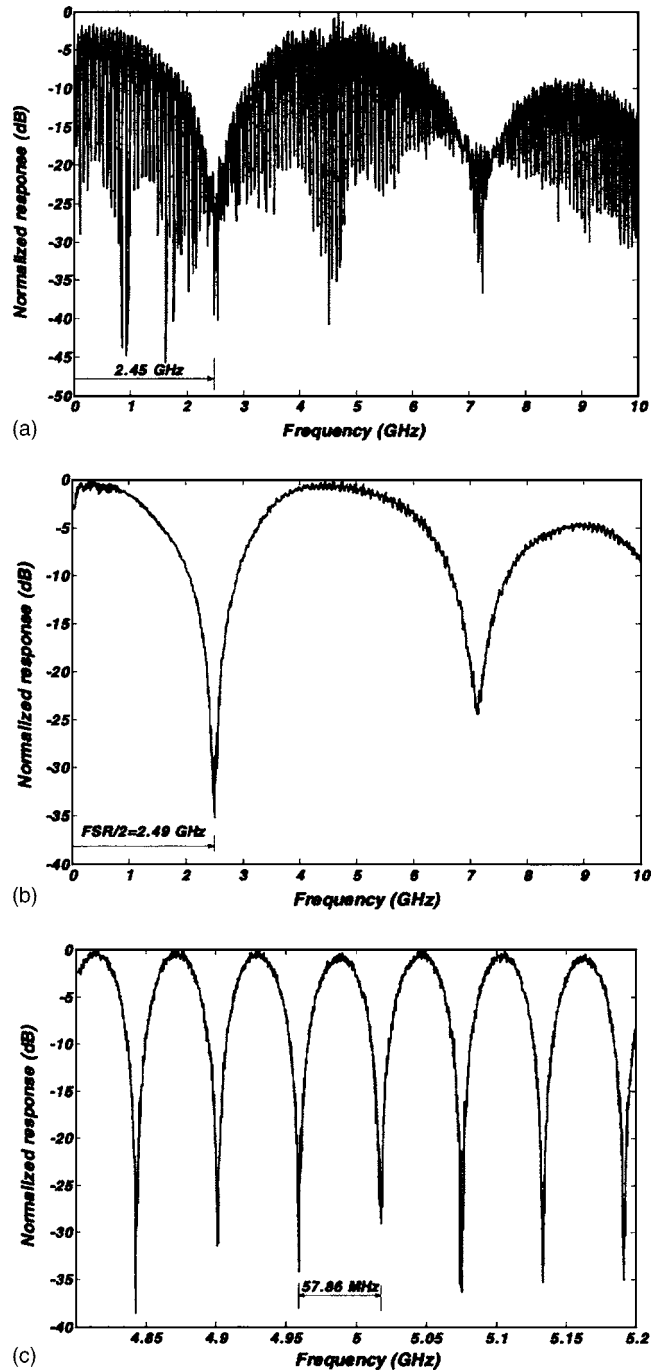


Fig. 4. (a) Measured filter response showing two simultaneous FSRs. (b) Filter response for the larger FSR measured by disconnecting arm 2 of the Sagnac loop. (c) Measured filter response enlarged  $\sim 5$  GHz.

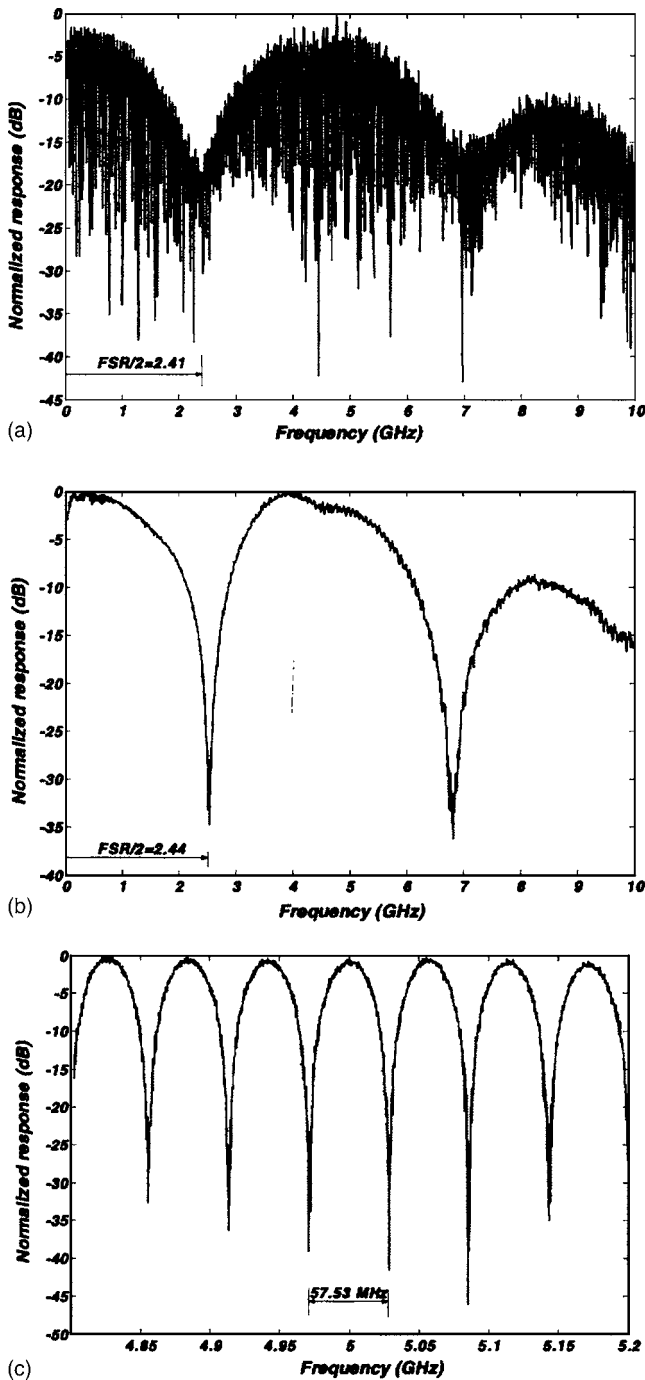


Fig. 5. (a) Measured filter response showing two simultaneous FSRs when the operation of the grating is shifted to a wavelength shorter by 0.1 nm. (b) Filter response for the larger FSR, measured by disconnecting arm 2 of the Sagnac loop, when the operation of the grating is shifted to a wavelength shorter by 0.1 nm. (c) Measured filter response enlarged at  $\sim 5$  GHz when the operation of the grating is shifted to a wavelength shorter by 0.1 nm.

#### 4. CONCLUSION

A novel, continuously tunable, photonic microwave notch filter configuration, yielding two simultaneous values of

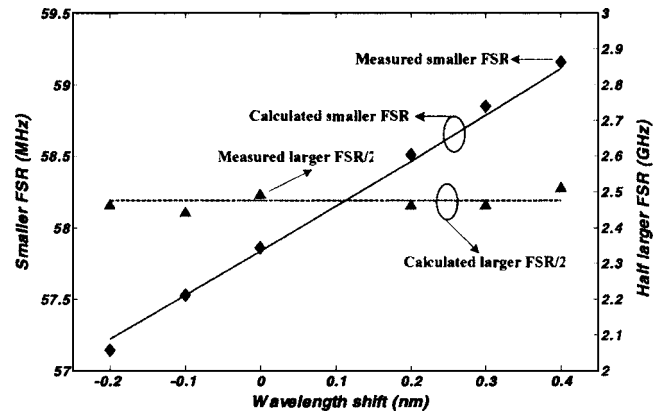


Fig. 6. Measured and calculated (solid line) larger and smaller FSR versus shift in the operating wavelength of the Hi-Bi LCFBG.

the FSR, has been proposed and demonstrated. The configuration uses a Hi-Bi LCFBG in a Sagnac loop. Measured results are presented to show tunability of the FSR and good agreement with the calculated FSR values. The proposed configuration can also be switched to a single FSR filter; moreover, this FSR value can be switched between two values.

Corresponding author G. Ning's e-mail address is ngxstone@pmail.ntu.edu.sg.

#### REFERENCES

1. J. Capmany, B. Ortega, D. Paster, and S. Sales, "Discrete-time optical processing of microwave signals," *J. Lightwave Technol.* **23**, 702–723 (2005).
2. D. Paster and J. Capmany, "Fibre optic tunable transversal filter using laser array and linearly chirped fibre grating," *Electron. Lett.* **34**, 1684–1685 (1998).
3. E. H. W. Chan, K. E. Alameh, and J. A. R. Minasian, "Photonics bandpass filters with high skirt selectivity and stopband attenuation," *J. Lightwave Technol.* **20**, 1962–1967 (2002).
4. D. B. Hunter, R. A. Minasian, and P. A. Krug, "Tunable optical transversal filter based on chirped gratings," *Electron. Lett.* **31**, 2205–2207 (1995).
5. A. R. Minasian, "Photonics signal processing of microwave signals," *IEEE Trans. Microwave Theory Tech.* **54**, 832–846 (2006).
6. W. Zhang, J. A. R. Williams, and I. Bennion, "Polarization synthesized optical transversal filter employing high birefringence fiber gratings," *IEEE Photon. Technol. Lett.* **13**, 523–525 (2001).
7. X. Yi, C. Lu, X. Yang, W. D. Zhong, W. Fang, L. Ding, and Y. X. Wang, "Continuously tunable microwave photonics filter design using high birefringence linear chirped grating," *IEEE Photon. Technol. Lett.* **15**, 754–756 (2003).
8. T. Erdogan, "Fiber grating spectra," *J. Lightwave Technol.* **15**, 1277–1294 (1997).
9. G. Ning, S. Aditya, Y. D. Gong, and P. Shum, "Tunable photonic microwave filter using fiber grating in a Sagnac loop," in *Asia Pacific Microwave Conference (APMC 2004)*, New Delhi, India (2004), pp. 209–210.
10. Z. Qin, Q. Zeng, X. Yang, D. Feng, L. Ding, G. Kai, Z. Liu, S. Yuan, X. Dong, and N. Liu, "Bidirectional grating wavelength shifter with a broad range tunability by using a beam of uniform strength," *IEEE Photon. Technol. Lett.* **13**, 326–328 (2001).